Heliyon 10 (2024) e23495

Contents lists available at ScienceDirect

Heliyon

journal homepage: www.cell.com/heliyon

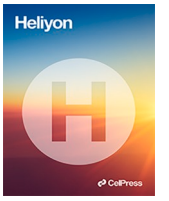

Establishment of novel ferroptosis-related prognostic subtypes correlating with immune dysfunction in prostate cancer patients

Dechao Feng [a,b,1,*], Zhouting Tuo [c,1], Jie Wang [a,1], Luxia Ye [d,1], Dengxiong Li [a], Ruicheng Wu [a], Wuran Wei [a], Yubo Yang [e,**], Chi Zhang [b,***]

[a] Department of Urology, Institute of Urology, West China Hospital, Sichuan University, Chengdu, 610041, China
[b] Department of Rehabilitation, The Affiliated Hospital of Southwest Medical University, Luzhou, 646000, China
[c] Department of Urology, The Second Affiliated Hospital of Anhui Medical University, Hefei, 230601, China
[d] Department of Public Research Platform, Taizhou Hospital of Zhejiang Province Affiliated to Wenzhou Medical University, Linhai, China
[e] Department of Urology, Three Gorges Hospital, Chongqing University, Wanzhou, Chongqing, 404000, China

ARTICLE INFO

Keywords:
Prostate cancer
Biochemical recurrence
Ferroptosis
Radical prostatectomy
Nonnegative matrix factorization
Molecular subtypes

ABSTRACT

Background: We aimed to identify two new prognostic subtypes and create a predictive index for prostate cancer (PCa) patients based on ferroptosis database.
Methods: The nonnegative matrix factorization approach was used to identify molecular subtypes. We investigate the differences between cluster 1 and cluster 2 in terms of clinical features, functional pathways, tumour stemness, tumour heterogeneity, gene mutation and tumour immune microenvironment score after identifying the two molecular subtypes. Colony formation assay and flow cytometry assay were performed.
Results: The stratification of two clusters was closely connected to BCR-free survival using the nonnegative matrix factorization method, which was validated in the other three datasets. Furthermore, multivariate Cox regression analysis revealed that this classification was an independent risk factor for patients with PCa. Ribosome, aminoacyl tRNA production, oxidative phosphorylation, and Parkinson's disease-related pathways were shown to be highly enriched in cluster 1. In comparison to cluster 2, patients in cluster 1 exhibited significantly reduced $CD4^+$ T cells, $CD8^+$ T cells, neutrophils, dendritic cells and tumor immune microenvironment scores. Only HHLA2 was more abundant in cluster 1. Moreover, we found that P4HB downregulation could significantly inhibit the colony formation ability and contributed to cell apoptosis of C4-2B and DU145 cell lines.
Conclusions: We discovered two new prognostic subtypes associated with immunological dysfunction in PCa patients based on ferroptosis-related genes and found that P4HB downregulation could significantly inhibit the colony formation ability and contributed to cell apoptosis of PCa cell lines.

* Corresponding author. Department of Urology, Institute of Urology, West China Hospital, Sichuan University, Chengdu, 610041, China.
** Corresponding author. Department of Urology, Three Gorges Hospital, Chongqing University, Wanzhou, Chongqing, 404000, China.
*** Corresponding author. Department of Rehabilitation, The Affiliated Hospital of Southwest Medical University, Luzhou, 646000, China.
E-mail addresses: fdcfenix@stu.scu.edu.cn, dechaofeng66@swmu.edu.cn (D. Feng), potatobo@126.com (Y. Yang), chizhang_swmu@126.com (C. Zhang).
[1] These authors contributed equally to this work.

https://doi.org/10.1016/j.heliyon.2023.e23495
Received 3 July 2023; Received in revised form 19 September 2023; Accepted 5 December 2023
Available online 9 December 2023

1. Introduction

Prostate cancer (Pca) is demonstrated to be one of the most frequent urinary tumors in elderly people [1,2] and contributed to about 1,414,259 new cases and 375,304 deaths worldwide in 2020 [3,4]. The burden of PCa was primarily held by older men, and it will rise as the global population ages [5–9]. Currently, PCa is treated with active surveillance, radical prostatectomy (RP) or radical radiotherapy (RT), androgen deprivation therapy, with the choice depending on the clinical stage, Gleason score, patient performance, and life expectancy [10]. BCR is an inevitable complication that affects in 27 %–53 % of localized patients undergoing RP and 10 %–70 % of localized patients receiving RT, respectively [11,12]. Additionally, the median time from metastasis to mortality is five years, while the average period from BCR to metastatic is eight years [6,11,12]. Therefore, the importance of screening BCR cases is highlighted by the fact that BCR marks a stage of transition in the development of PCa. Geographical and clonal genetic diversity in PCa can serve as examples of its clinical variability [13]. Researchers will have access to a variety of genetic and clinical variables to approach precision medicine at several levels with the completion of the cancer genome atlas (TCGA).

In 2012, ferroptosis was proposed as a type of nonapoptotic cell death which required iron and lipid peroxidation [14]. Numerous biological processes, including maturation, immunology, cancer initiation, progression, and suppression, have been connected to ferroptosis [11,15–18]. The complex biochemical pathways behind ferroptosis are driven by an imbalance of antioxidant, iron, and lipid dynamics [14,17]. In terms of the application of ferroptosis in PCa therapy, macromolecular enzymes (ChaC glutathione-specific γ-glutamylcyclotransferase 1, valosin-containing protein and mitochondrial 2,4-dienoyl-CoA reductase), small-molecule inducers (erastin, sulfasalazine, sorafenib, glutamate, cisplatin and BAY87–2243) and gene-related treatment (flubendazole, pannexin 2, PCa-associated transcription 1 and transcription factor AP-2γ) are possible options [19]. Even though PCa treatment based on ferroptosis has made some progress, the subject is still in its infancy, and ferroptosis-targeting nanomaterials, gene therapy and medications may hold great potential [19]. The FerrDB database created by Zhou et al. is the first manually curated database on ferroptosis regulators and markers as well as connections between ferroptosis and diseases (including 108 drivers, 69 suppressors, 35 inducers, 41 inhibitors, 111 indicators, and 95 ferroptosis-disease associations) [20]. We identified important ferrroptosis-related genes in PCa based on their findings, developed and validated novel molecular subtypes, and then utilised a prognostic indicator for PCa patients to boost the undertstanding of ferroptosis in this disease and enhance therapeutic decision-making.

2. Methods

2.1. Screening genes and identifying molecular subtypes

We used the gene matrix of PCa patients from the TCGA database as a training test. To validate the findings obtained in the TCGA database, four gene expression omnibus (GEO) datasets (GSE46602 [21], GSE32571 [22], GSE62872 [23], and GSE116918 [24]) and MSKCC 2010 (http://www.cbioportal.org/) [25] were used. Our earlier studies [6,12,26] showed the detailed method of gene matrix in the TCGA database and GEO datasets. In addition, the FerrDB database yielded 475 genes associated with human ferroptosis [20]. In order to find potential genes for cluster analysis, we firstly intersected the differentially expressed genes (DEGs) and BCR-free survival associated genes in the TCGA database with ferroptosis-related genes. DEGs were defined as |logFC| >0.5 and p.adj. < 0.01. Using the R package "survival," the P value of BCR-free survival was limited to less than 0.05. The differential expression of potential genes between tumour and normal samples was validated using GSE46602 [21], GSE32571 [22], and GSE62872 [23]. The 430 PCa samples in the TCGA database were then divided into many subtypes using the candidate genes and the nonnegative matrix factorization (NMF) algorithm. Among these subtypes, the forms of two subtypes (cluster 1 and cluster 2) were significantly associated with BCR-free survival and were further examined. The same candidate genes were used to validate the results in GSE46602 [21], GSE116918 [24], and MSKCC 2010 [25] using the NMF algorithm.

We investigate the differences between cluster 1 and cluster 2 in terms of clinical features, functional pathways [27,28], tumour stemness, tumour heterogeneity, gene mutation, tumour immune dysfunction and exclusion (TIDE) score, and tumour immune microenvironment score after identifying the two molecular subtypes. The ESTIMATE algorithm assessed the overall TME using the Wilcoxon rank sum test, while the TIMER method assessed the immune cells [29–31]. The TIDE algorithm was used to estimate the potential response to immune checkpoint blockade (ICB) therapy [32]. A high TIDE score correlates with poor ICB efficacy. For tumor stemness indexes, differentially methylated probes-based stemness scores (DMPss), DNA methylation-based stemness scores (DNAss), enhancer elements/DNA methylation-based stemness scores (ENHss), epigenetically regulated DNA methylation-based stemness scores (EREG-METHss), epigenetically regulated RNA expression-based stemness scores (EREG.EXPss) and RNA expression-based stemness scores (RNAss), were used to evaluate the differences of stemness features between two clusters using the Wilcoxon rank sum test [33]. Similarly, homologous recombination deficiency (HRD) [34], loss of heterozygosity (LOH) [34], neoantigen (NEO) [34], tumour ploidy [34], tumour purity [34], mutant-allele tumour heterogeneity (MATH) and tumour mutation burden (TMB) [35], and microsatellite instability (MSI) [36] were also compared. The detailed methods for the above indicators could be seen in our previous studies [8,37–42].

2.2. Developing prognositc index

We created a predictive indicator for PCa patients in order to improve therapeutic applicability of our molecular subtypes. We utilised the R package "limma (version 3.40.6)" to collect DEGs in the TCGA database between clusters 1 and 2. DEGs were defined as absolute logFC values more than 0.5 and adjusted P value less than 0.01. Subsequently, lasso and Cox regression were used to

constructed the gene signature and prognositc index, namely risk score (0.5025*HUNK+0.6309*CCDC85B+0.4482*PRDM1+0.3449*SLITRK5+0.6267*CD209-0.4313*ZNF676-0.5000*NLGN4Y). GSE46602 [15] and MSKCC 2010 [19] were used to validate the prognostic efficacy of this risk score. Fig. 1 presents the overall flowchart of this study.

2.3. Colony formation assay and flow cytometry assay

Our previous study demonstrated that Bacitracin's suppression of P4HB reduced cell proliferation and made bladder cancer cells more sensitive to gemcitabine through inducing apoptosis and the PERK/eIF2/ATF4/CHOP pathways [43]. Moreover, our another study showed that P4HB downregulation could significantly inhibit the cell proliferation of six PCa cell lines using CCK8 assay [44]. In this study, we further explored the effect of P4HB on PCa cell lines. For colony formation assay, the C4-2B and DU145 cells were seeded in 12-well plates at a density of 1000 cells/well. After 10–14 days of incubation, the colonies were fixed with 4 % paraformaldehyde and stained with 0.1 % crystal violet for 30 min [43]. In addition, cell apoptosis assay was analyzed using a specific detection kit (Annexin V-APC/7-AAD Apoptosis Kit; cat. No: E-CK-A218, Elabscience, www.elabscience.cn) according to its instruction. Methods of Cell culture, small interfering RNA and other basic information could be seen in our previous study [44].

2.4. Statistical analysis

We applied the Wilcoxon test when a distribution was out of the ordinary. The survival analysis, shown as a Kaplan-Meier curve, was performed using the log-rank test. The two-sided $p < 0.05$ was chosen as statistical significance level. The following were the significant marks: not significant (ns), $p > 0.05$; *, $p < 0.05$; **, $p < 0.01$; ***, $p < 0.001$.

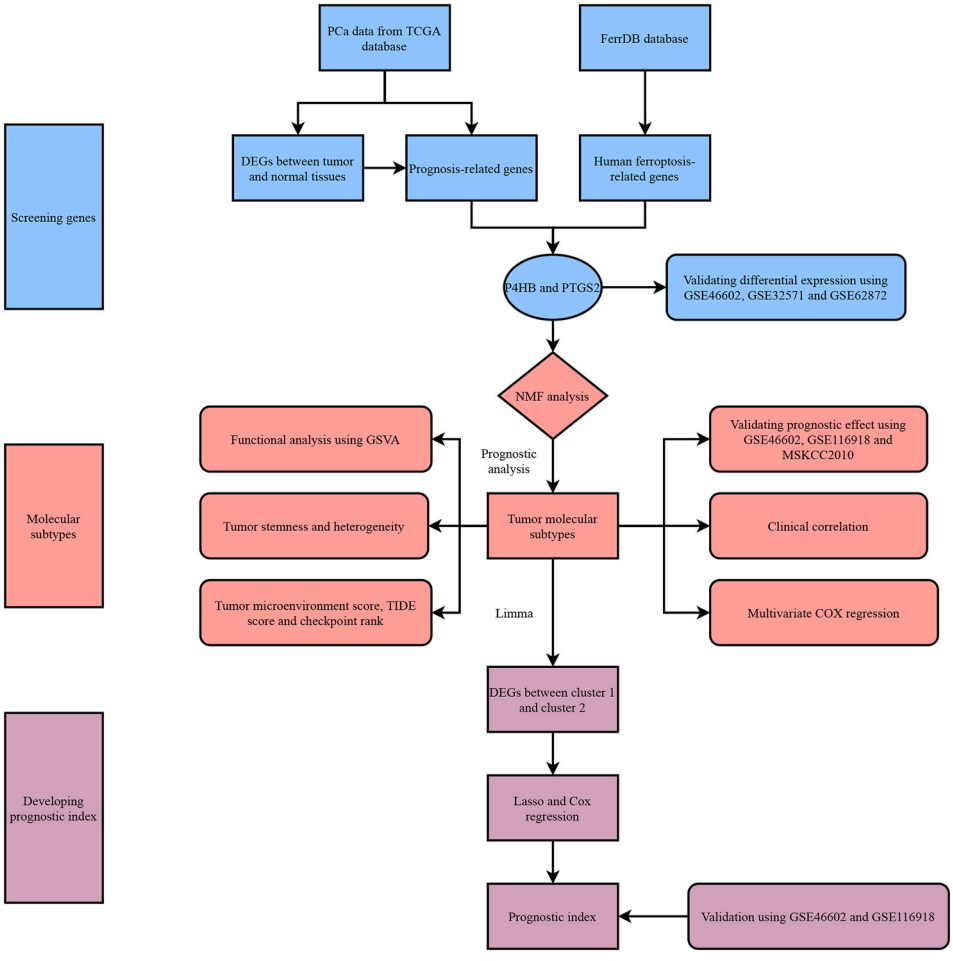

Fig. 1. The flowchart of this study. PCa = prostate cancer; DEGs = differentially expressed genes; NMF = nonnegative matrix factorization; GSVA = gene set variation analysis; TIDE = tumor immune dysfunction and exclusion; TCGA = the cancer genome atlas.

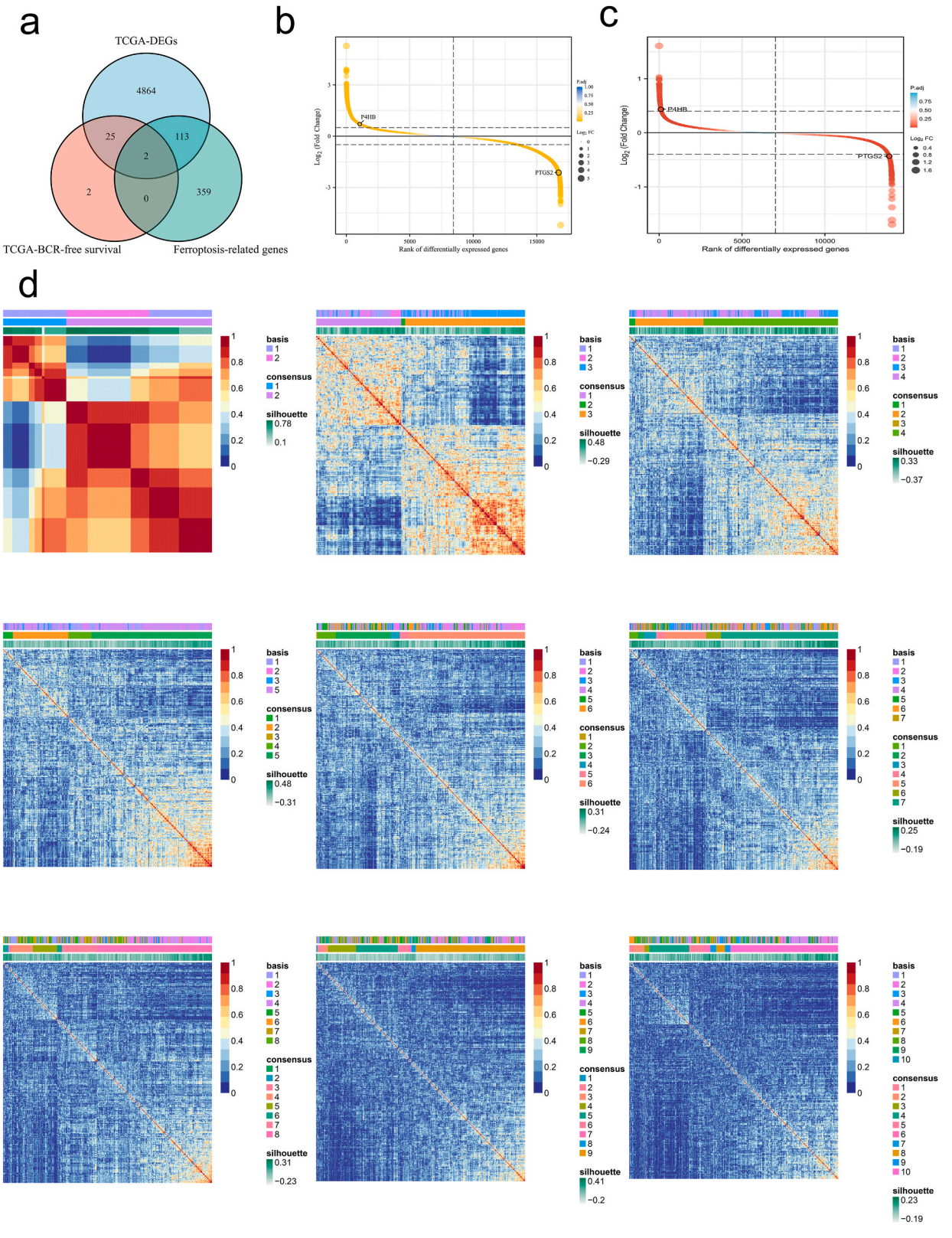

(caption on next page)

Fig. 2. Identification of molecular subtypes. (a). Venn plot showing the intersection of DEGs, prognosis-related genes and ferroptosis-related genes; (b). ranking plot of DEGs showing the expression level of P4HB and PTGS2 between tumor and normal samples in the TCGA database; (c) ranking plot of DEGs showing the expression level of P4HB and PTGS2 between tumor and normal samples in the GEO datasets; (d) the results of heatmaps using NMF algorithm. DEGs = differentially expressed genes; NMF = nonnegative matrix factorization; TCGA = the cancer genome atlas; BCR = biochemical recurrence; GEO = gene expression omnibus.

3. Results

3.1. Screening genes and identifying molecular subtypes

The TCGA database was utilised to find DEGs in 498 tumour and 52 normal PCa samples, and 430 PCa patients undergoing RP with complete BCR data were used to identify prognosis-related genes. P4HB and PTGS2 were discovered by combining DEGs, BCR-free survival related genes, and ferroptosis-related genes (Fig. 2a). P4HB was upregulated in tumour samples while PTGS2 was downregulated, according to the TCGA database (Fig. 2b). The results were validated again using 360 tumour and 209 normal samples from the three GEO datasets (Fig. 2c) [21–23]. Based on P4HB and PTGS expression, we identified nine potential PCa subtypes using the NMF method (Fig. 2d). Fig. S1a depicted the NMF rank survey. The stratification of two clusters among the subtypes was closely connected to BCR-free survival (Fig. 3a), which was confirmed in the other three datasets (Fig. 3b; [21]; Fig. 3c; [24]; Fig. 3d; [25]). The two clusters' baseline characteristics were balanced (Table 1). Furthermore, multivariate Cox regression analysis revealed that this classification was an independent risk factor for patients with PCa (Fig. 3e). The GSVA analysis revealed that ribosome, aminoacyl tRNA biosynthesis, oxidative phosphorylation, and Parkinson's disease-related pathways were highly enriched in cluster 1, whereas circadian rhythm, leishmania infection, dorsoventral axis formation, cytokine-cytokine receptor interaction, and arrhythmogenic right ventricular cardiomyopathy were highly enriched in cluster 2. (Fig. 3f). The waterfall plot revealed that TP53 was the most frequently mutated gene in PCa, while APC, CSMD1, NYNRIN, and USP31 were significantly different between clusters 1 and 2. (Fig. 3g).

In terms of tumour heterogeneity and stemness, cluster 2 had significantly lower LOH, tumour purity, TMB, DMPss, and RNAss than cluster 1. (Fig. 3h). In cluster 2, we split the patients into two groups based on the median MSI score. Those with high-score MSI had a greater risk of BCR than patients with low-score MSI (Fig. 3i). In cluster 2, similar results were obtained in terms of HRD score (Fig. 3j). In comparison to cluster 2, patients in cluster 1 exhibited significantly reduced $CD4^+$ T cells, $CD8^+$ T cells, neutrophils, dendritic cells, stromal score, immunological score, ESTIMATE score, and TIDE score (Fig. 4a–c). The majority of immunological checkpoints were more abundant in Cluster 2, and the top three genes were VTCN1, TNFSF15, and CD200 (Fig. 4d). Only HHLA2 was found to be more abundant in Cluster 1. (Fig. 4d).

3.2. Developing prognostic index

There were 1963 DEGs found between clusters 1 and 2. (Fig. 5a). We used lasso regression and set the lambda value to 0.03 (Fig. 5b) to get a total of 29 genes (Fig. 5c). These 29 genes were substantially linked with BCR-free survival in the univariate Cox regression (Fig. 5d). After multivariate Cox regression, the prognostic signature and risk score were built using CD209, HUNK, CCDC85B, ZNF676, NLGN4Y, PRDM1, and SLITRK5 (Fig. 5e). Fig. 5a also depicted the expression of these genes between two clusters. The established risk score demonstrated moderate diagnostic accuracy for BCR (Fig. 5f), and this ability remained steady throughout time (Fig. 5g). According to the value of the risk score, PCa patients were separated into upper third and lower third groups in the TCGA database. The upper third group was at a higher risk of BCR than the lower third group (Fig. 5h). GSE46602 (Fig. 5i) [21] and MSKCC 2010 (Fig. 5j) [25] validated this finding.

3.3. Colony formation assay and flow cytometry assay

We found that P4HB downregulation could significantly inhibit the colony formation ability (Fig. 6a) and contributed to cell apoptosis (Fig. 6b) of C4-2B and DU145 cell lines.

4. Discussion

Age and inflammation are considered as important risk factors of various cancers, including PCa [3,45–54]. Ferroptosis is an iron-dependent, lipid-peroxidation-induced programmed cell death that is followed by significant iron accumulation, lipid peroxidation, an increase in reactive oxygen species (ROS) [14,55–57]. Cellularly, it can be identified by a contracted mitochondrial membrane, a rupture in the outer mitochondrial membrane, and a reduction (or disappearance) of the mitochondrial crest [58,59]. In this study, we identified two novel subtypes based on ferroptosis-related P4HB and PTGS2. Ferroptosis and PCa have both been extensively researched in terms of PTGS2. Cyclooxygenase-2 (COX-2), a rate-limiting enzyme in the manufacture of prostaglandins (PGs), is encoded by the gene PTGS2 [60]. PTGS2 has been identified as a ferroptosis-related biomarker in a variety of disorders [61,62], including PCa [63], and COX-2/PGE2 has been linked to ferroptosis [64]. Furthermore, several studies have identified elevated COX-2 expression in PCa patients [65–67], and COX-2 inhibitors have been proven to play a protective effect in PCa progression [68,69]. On the other hand, little study has been done on P4HB in the context of PCa or ferroptosis. In the endoplasmic reticulum (ER), P4HB protein acts as a molecular chaperone by the correction of improperly folded proteins in response to ER stress [70]. Except for

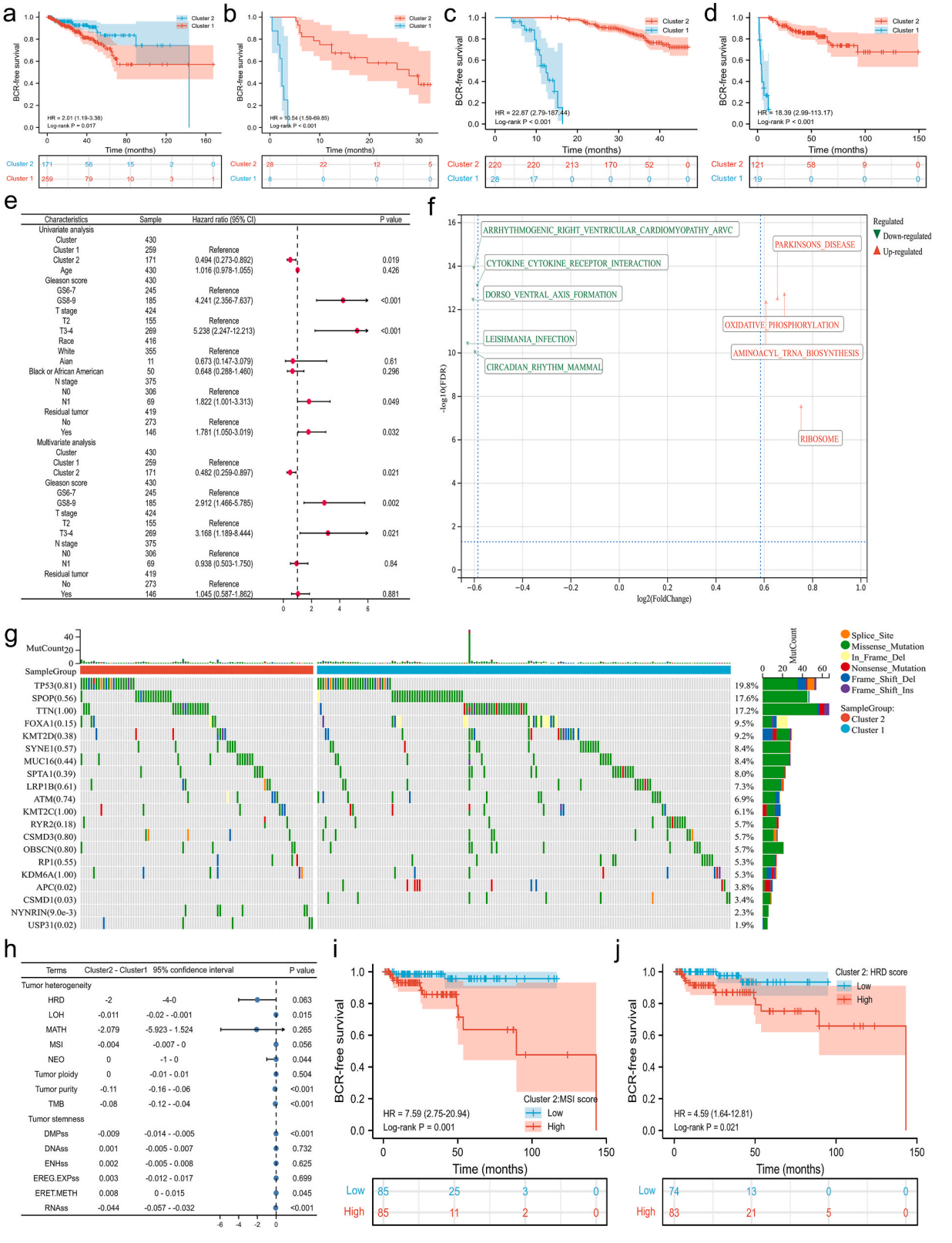

(caption on next page)

Fig. 3. Clinical applications, functional pathways, mutation genes, tumor heterogeneity and stemness of identified two clusters. (a). Kaplan-Meier curve showing the survival differences of two clusters in the TCGA database; (b). Kaplan-Meier curve showing the survival differences of two clusters in the GSE46602; (c). Kaplan-Meier curve showing the survival differences of two clusters in the GSE116918; (d). Kaplan-Meier curve showing the survival differences of two clusters in the MSKCC 2010; (e). forest plot showing the results of univariate and multivariate Cox regression analysis; (f). volcano plot showing the fucantional pathways of the two clusters using GSVA method; (g). Oncoplot showing the differential frequency of top 20 genes between two clusters; (h). forest plot showing the comparison of two clusters for tumor hetergeneity and stemness; (i) Kaplan-Meier curve showing the survival differences of high and low score of MSI in the cluster 2; (j). Kaplan-Meier curve showing the survival differences of high and low score of HRD in the cluster 2. TCGA = the cancer genome atlas; BCR = biochemical recurrence; DMPss = differentially methylated probes-based stemness scores; DNAss = DNA methylation-based stemness scores; ENHss = enhancer elements/DNA methylation-based stemness scores; EREG-METHss = epigenetically regulated DNA methylation-based stemness scores; EREG.EXPss = epigenetically regulated RNA expression-based stemness scores; RNAss = RNA expression-based stemness scores; HRD = homologous recombination deficiency; LOH = loss of heterozygosity; NEO = neoantigen; MATH = mutant-allele tumor heterogeneity; TMB = tumor mutation burden; MSI = microsatellite instability; HR = hazard ratio.

Table 1
The baseline features of two clusters in prostate cancer patients in the TCGA database.

Characteristics	Cluster 1	Cluster 2	P value
Samples	259	171	
Age, mean ± SD	60.81 ± 6.68	61.12 ± 6.89	0.640
Gleason score, n (%)			0.643
GS6	27 (6.3 %)	12 (2.8 %)	
GS7	120 (27.9 %)	86 (20 %)	
GS8	36 (8.4 %)	23 (5.3 %)	
GS9	76 (17.7 %)	50 (11.6 %)	
T stage, n (%)			0.706
T2	92 (21.7 %)	63 (14.9 %)	
T3	158 (37.3 %)	103 (24.3 %)	
T4	6 (1.4 %)	2 (0.5 %)	
Race, n (%)			0.090
Asian	9 (2.2 %)	2 (0.5 %)	
Black or African American	35 (8.4 %)	15 (3.6 %)	
White	205 (49.3 %)	150 (36.1 %)	
N stage, n (%)			0.256
N0	174 (46.4 %)	132 (35.2 %)	
N1	45 (12 %)	24 (6.4 %)	
Residual tumor, n (%)			1.000
No	164 (39.1 %)	109 (26 %)	
Yes	88 (21 %)	58 (13.8 %)	

SD: standard deviation.

our previous studies [43,44], several studies showed the close relationship between P4HB expression and diseases of the kidney and liver [43,71–73] and Pan et al. identified circular P4HB as a novel ferroptosis suppressor [74]. Moreover, we found that P4HB downregulation could significantly inhibit the colony formation ability and contributed to cell apoptosis of C4-2B and DU145 cell lines.

Our results suggested that cluster 1 had a worse prognosis than cluster 2, most likely because the two clusters had different enriched pathways. In comparison to cluster 2, ribosome, aminoacyl tRNA synthesis, and oxidative phosphorylation pathways were more prevalent in cluster 1. It is generally known that cancer cells need to produce a lot of protein in order to proliferate quickly and survive [75]. A higher degree of proliferation and invasion demand for PCa cells in cluster 1, which is correlated with a worse prognosis, may be reflected by the concentration of protein-synthesis-related pathways in cluster 1. Surprisingly, oncogene and tumor suppressor gene alterations that result in excessive ribosome synthesis have a significant impact in the development and spread of cancer [76]. A study on the nucleolar N-terminal shortened version of netrin 1 found that more mature ribosomes promote the malignant phenotype [77], which was also found in lymphoma [78]. These findings may help to explain our results that the enrichment of pathways related to protein synthesis is a biological indicator of cluster 1's worse prognosis and a likely contributor to the higher degree of malignancy. The Warburg effect revealed that even in well-oxygenated cancer cells, glycolysis was increased in comparison to normal cells, dispelling the popular notion that oxidative phosphorylation was typically down-regulated in cancer [79,80]. PCa cells were less reliant on glycolysis and more reliant on oxidative phosphorylation than most other solid cancers [81]. Different oxidative phosphorylation pathways may therefore contribute to the poor prognosis of cluster 1. In cluster 2, pathways involving cytokine-cytokine receptor interaction and circadian rhythm were also more prevalent. It is commonly recognized that circadian rhythm can regulate a variety of human behaviors, physiological processes, and activities [82–84], and as a result, circadian rhythm disruption has been linked to poor health and many disorders, including PCa [85,86]. Chronotherapy based on circadian rhythm has proven to be extremely effective in managing PCa outcomes [87]. Particularly ferroptosis may function as a potential mechanism for the tumor-promoting effect of circadian rhythm disruption. According to a recent study, ferroptosis is promoted in cancer cells both in vitro and in vivo by clockophagy, which is the selective autophagic degradation of the circadian clock regulator ARNTL/BMAL1 [88]. Because ferroptosis is also present in cluster 2, a regular circadian rhythm may have a substantial role in enhancing the prognosis of PCa patients. The enrichment of related pathways may indicate elevated immune cell activity in cluster 2, which will be investigated

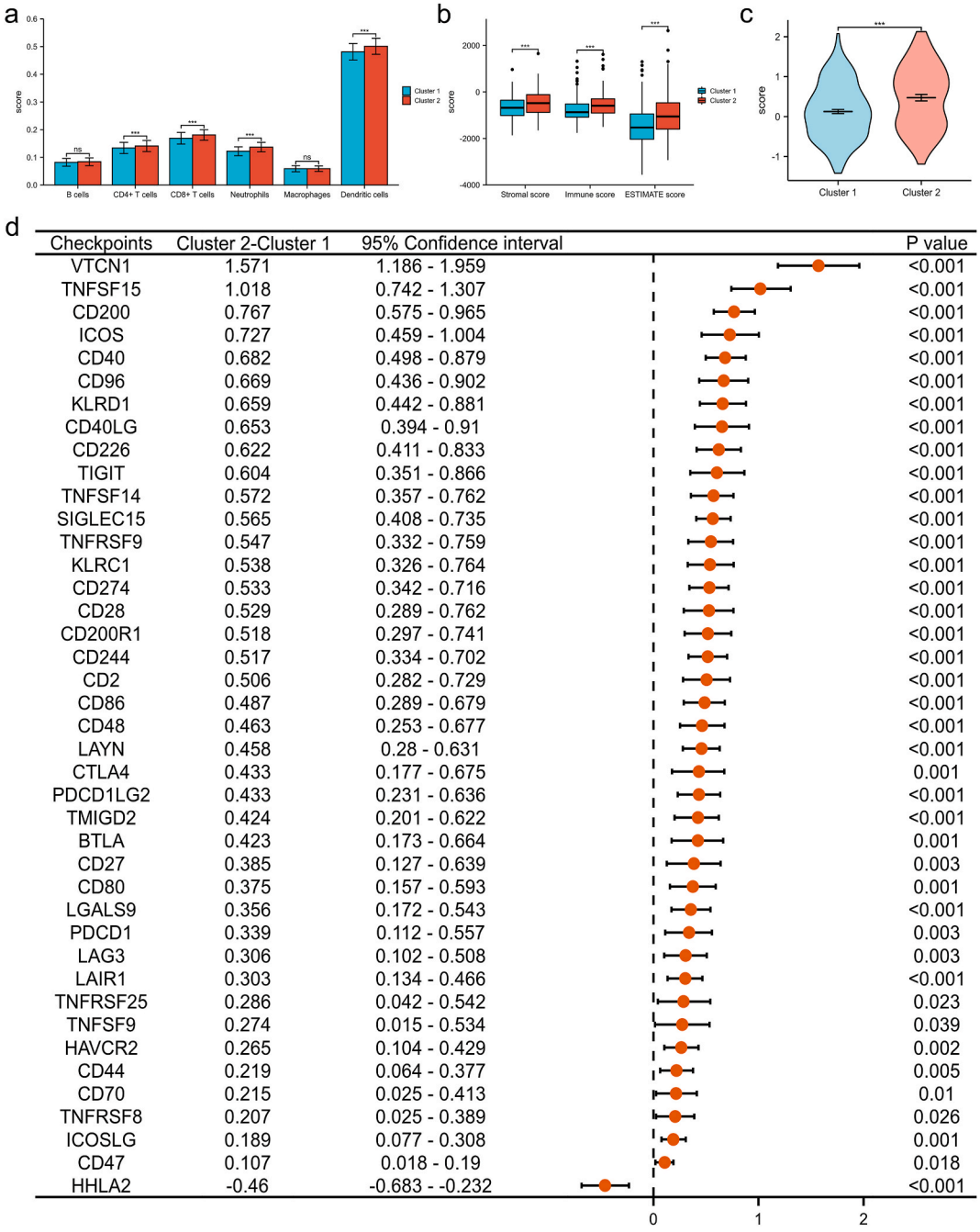

Fig. 4. Immune-related assessment of two clusters. (a). bar chart showing the differencs of immune cells between two clusters; (b). bar chart showing the differencs of tumor immune microenvironment scores between two clusters; (c). bar chart showing the differencs of TIDE scores between two clusters; (d). forest plot showing the comparison of two clusters for immune checkpoints. TIDE = tumor immune dysfunction and exclusion.

next, in terms of cytokine receptor interactions.

Another frequent aspect of PCa development is genomic instability, which may be one of the most important aspects of carcinogenesis. An often-changed tumor suppressor gene in PCa, particularly in metastatic castration-resistant PCa (mCRPC), is TP53, which controls cell cycle arrest and encodes proapoptotic protein [89]. TP53 mutations are present in about 8 % of locally advanced PCa cases, while they are present in 27 % of metastatic castration-sensitive PCa cases and 50 % of mCRPC cases [90–92], highlighting the importance of TP53 mutation in more aggressive PCa. According to Laere et al., PCa patients with TP53 mutations tend to be more aggressive and have worse outcomes [93]. With a 19.8 % mutation frequency in TP53, our results confirmed this. From the standpoint

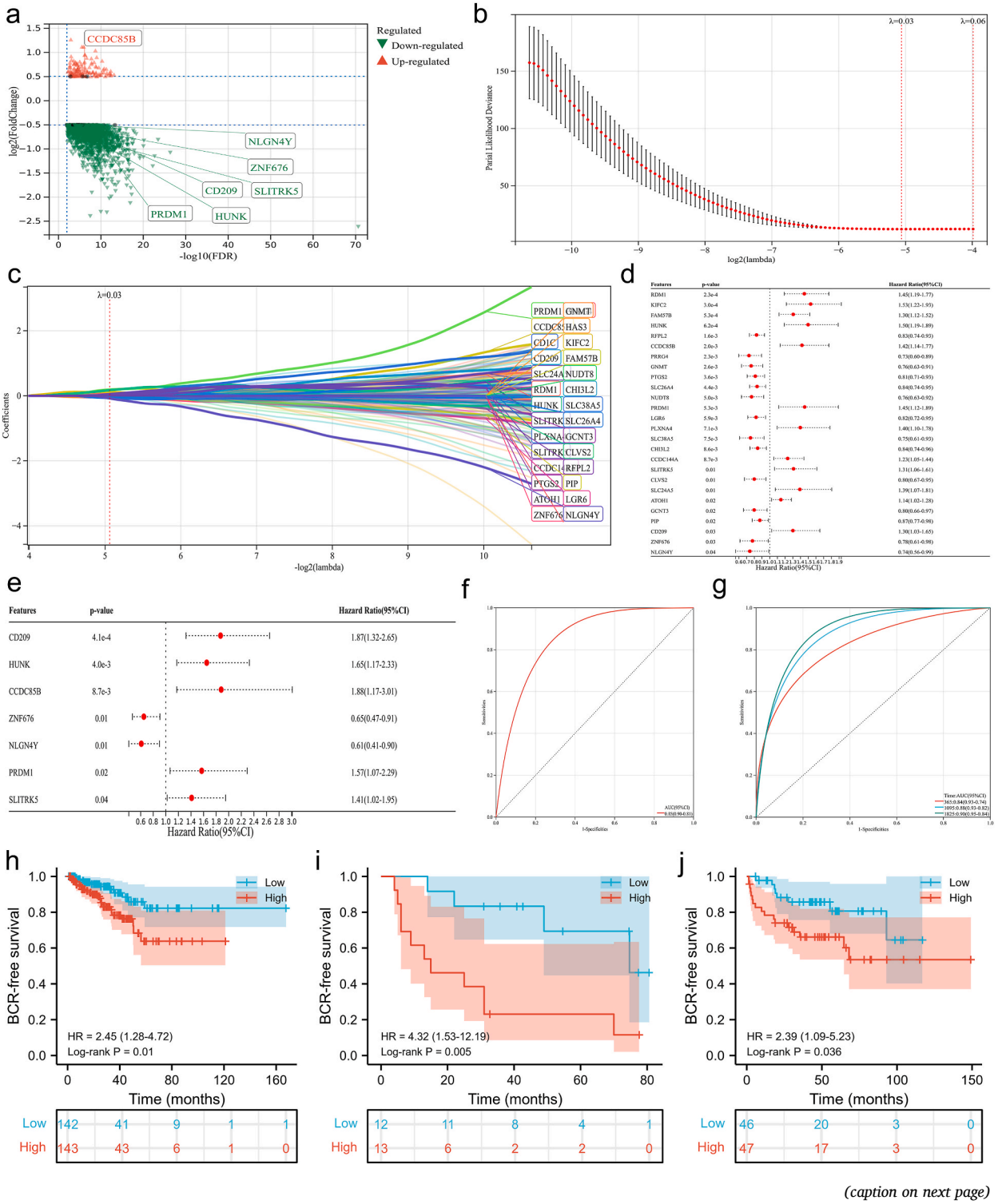

(caption on next page)

Fig. 5. Developing prognostic index. (a). volcano plot showing the DEGs between cluster 1 and cluster 2; (b). screening the lambda values using Lasso regression; (c). trajectory chart showing 29 DEGs when lambda equals 0.03; (d). forest plot showing the results of 29 DEGs using univariate Cox regression; (e) forest plot showing the results of multivariate Cox regression; (f) ROC curve showing the diagnostic accuracy of risk score established by multivariate Cox regression in distinguishing BCR from no BCR; (g). time-dependent ROC curve showing the diagnostic accuracy of risk score established by multivariate Cox regression in distinguishing BCR from no BCR; (h). Kaplan-Meier curve showing the survival differences of upper third and lower third patients in the TCGA database; (i). Kaplan-Meier curve showing the survival differences of upper third and lower third patients in the GSE46602; (j). Kaplan-Meier curve showing the survival differences of upper third and lower third patients in the MSKCC 2010. DEGs = differentially expressed genes; TCGA = the cancer genome atlas; BCR = biochemical recurrence; ROC = receiver operating characteristic curve; HR = hazard ratio.

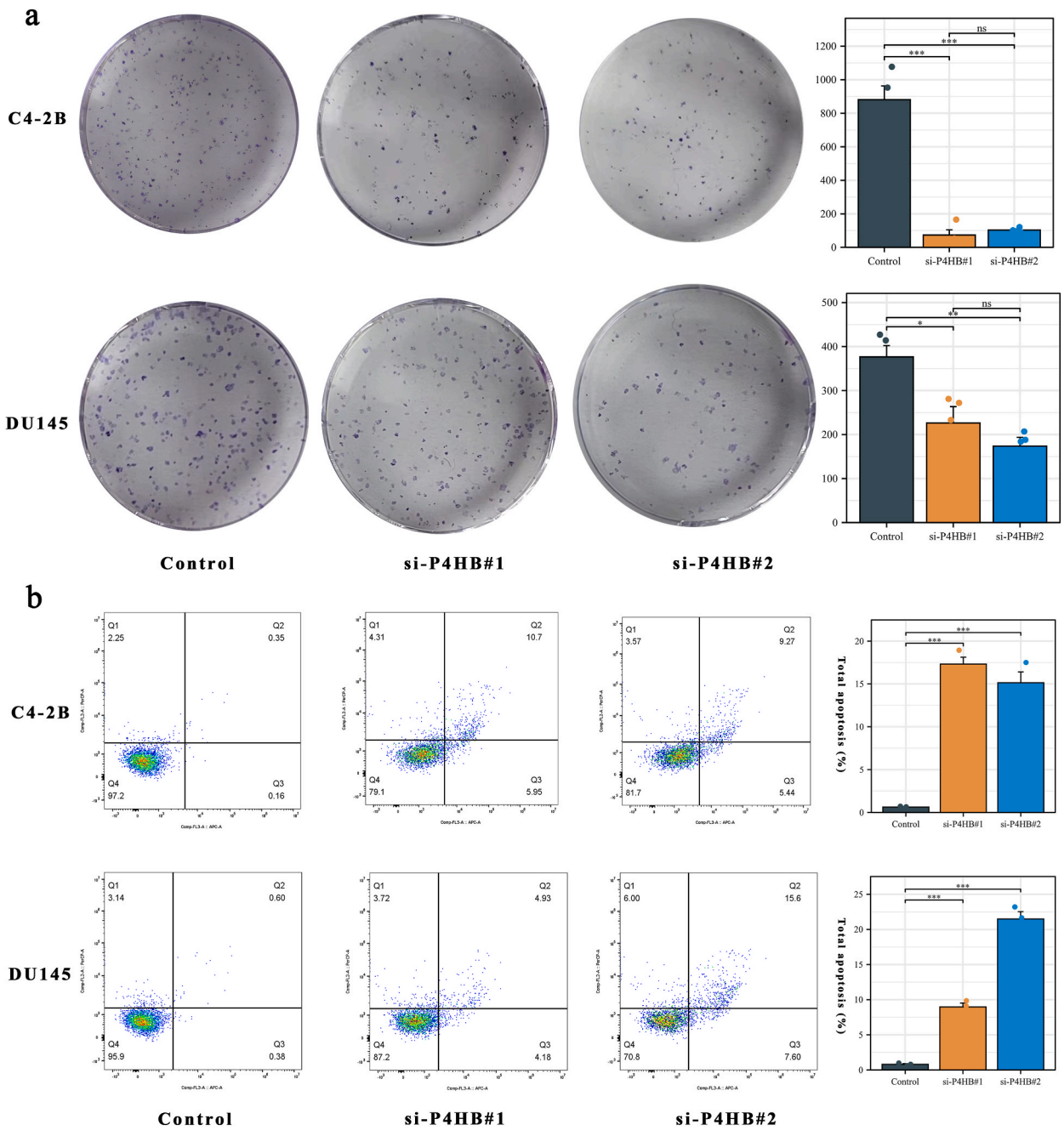

Fig. 6. Colony formation assay and flow cytometry assay using C4-2B and DU145 cell lines. (a) colony formation assay; (b) cell apoptosis assay.

of the mutant landscape, inactivation of tumor suppressor genes may result in more aggressive PCa, resulting in a worse prognosis in cluster 1 patients.

LOH, as a chromosomal event, is closely linked with chromosomal instability, which has been identified as a characteristic of cancer and a cause of poor prognosis [94]. Furthermore, the diversity in somatic copy number changes that provides the variance required for tumor evolution [95]. 6q, 7q, 8p, 10q, 13q, 16q, 17q, and 18q chromosome loss is well documented in PCa [96], and metastatic PCa demonstrated greater genomic instability than primary PCa [97]. In line with these conclusions, we found that LOH was significantly higher in cluster 1. TMB in cluster 1 was also higher than in cluster 2. While TME is widely used to forecast the effectiveness of immunotherapy, TMB represents the total number of genetic mutations from a biological perspective. Generally speaking, cluster 1 could be more malignant and have a poorer prognosis than cluster 2. Additionally, due to the lack of high-fidelity repair to DNA double strand breaks, HRD will result in increased genomic alternations [98]. HRD was frequently detected in PCa as a characteristic of various malignancies [99,100]. Prior to the poly (ADP-ribose) polymerases (PARP) inhibitor (PARPi) therapy [101], HRD detection was used to evaluate the sensitivity of breast and ovarian cancer to PARPi therapy [102]. In recent years, multiple PARPis have been studied in PCa patients at various stages, and they have shown surprisingly good performance [100], showing that genetically based targeted therapy in PCa is a potential option. Based on the median HRD score, we divided Cluster 2 into two groups, with high-scoring HRD patients having a higher likelihood of BCR. The two subgroups we identified may also provide a fresh approach for the treatment of PCa patients, particularly those with metastases, as a result of HRD's strong predictive power for PARPi effectiveness. MSI is the insertion or deletion of repeating units from DNA tracts [103]. MSI-high states have been linked to increased synthesis of various newly generated antigens, hence boosting the anticancer immune response [104–106]. MSI-high PCa, like other solid tumors, may respond better to immune checkpoint blockade [107]. As a result, the median MSI score-different subgroups observed in cluster 2 may also separate specific treatment sensitive patients for PCa immunotherapy.

Interestingly, Wang et al. reported that activated T cells, particularly $CD8^+$ T cells, increased IFN- production and caused lipid peroxidation and consequent ferroptosis in tumor cells [108]. Furthermore, increased ferroptosis improved immunotherapy efficacy [108]. As a result, we hypothesized that the better prognosis in cluster 2 was due to increased T cell numbers, which led to antitumor-specific ferroptosis. Other immune cells highly infiltrated in cluster 2 might also suggest stronger anti-tumor immunity and a better prognosis. In addition, the immunological score of cluster 2 was higher than that of cluster 1, which could indicate that cluster 2 had more tumor infiltrating immune cells and thus more anticancer immune activity. On the contrary, despite having more active immune functions, cluster 2 had a higher TIDE score than cluster 1, indicating a more sensitive response to immunotherapy than cluster 1 [32]. This finding could imply that immunosuppression was the primary cause of cluster 1's poor prognosis, and hence that cluster 1 would respond better to immunotherapy involving immune activation. Our findings on tumor stemness also supported this hypothesis. TMB and tumor purity were found to be considerably greater in cluster 1. TMB-high has been proposed as a leading candidate biomarker for predicting ICB response and identifying patients who will benefit the most, based on the premise that antigenic peptides from enhanced mutant protein may generate immunogenic novel antigens [109,110]. A higher TMB score may also indicate that patients in cluster 1 respond better to immunotherapy. Furthermore, higher tumor purity in cluster 1 may indicate less infiltration of tumor-associated immune cells, resulting in greater immunosuppression and a worse prognosis. Furthermore, our immune checkpoint research revealed variations in immune activity across clusters 1 and 2. Across the two clusters, VTCN1 was the most differentially expressed immune checkpoint molecule. Interestingly, the coinhibitory molecule VTCN1 is an important member of the B7 family, primarily suppressing T cell activation by down-regulating IL-2 production and increasing $CD4^+$ and $CD8^+$ T cell cycle arrest [111]. VTCN1 had a negative immunomodulatory effect in PCa and was an independent poor prognostic factor for PCa [112]. However, this does not corroborate our findings (patients in cluster 2 with more active immune functions and a better prognosis), and we believed epigenetic alteration was crucial. HHLA2 was the only molecule higher elevated in cluster 1 compared to the most differentially expressed immune checkpoints. Overall, multiple studies have shown that HHLA2 is a T cell coinhibitory molecule, primarily inhibiting T cell proliferation as well as T cell-associated cytokine responses [113], which is consistent with our finding that the pathway involving cytokine-cytokine receptor interactions was less enriched in cluster 1. Interestingly, previous research found that elevated HHLA2 expression in lung, breast, and osteosarcoma was related with worse prognostic characteristics [114–116], offering yet another reason for cluster 1's poor prognosis. To summarize, whereas PCa cells upregulate PD-L1 expression to avoid immune surveillance, the majority of PCa patients are not responsive to long-term immunotherapy [117]. Our findings revealed that ferroptosis plays a crucial role in PCa immunotherapy and offered possible therapeutic targets, potentially opening up new avenues for PCa immunotherapy.

Finally, we created a predictive index by combining 7 DEGs from cluster 1 and cluster 2. NLGN4Y (a neuron-derived protein) was identified as a unique negative regulator of PCa development and BCR [118]. In vitro, Gong et al. found that reduced NLGN4Y expression was related with increased BCR risk [118]. Hu et al. also validated PRDM1 overexpression in PCa and discovered that silencing PRDM1 decreased PCa cell proliferation, migration, and invasion [119]. Although there was no clear evidence for their participation in PCa, CD209, HUNK, CCDC85B, ZNF676, and SLITRK5 were identified as elevated malignant phenotype- and poor prognosis-associated variables in many cancer types [120–125]. In summary, these genes had direct or underlying association to BCR, and the developed risk score based on them also demonstrated reasonable predictive accuracy of BCR, indicating the potential utility of the prognostic index in clinical practice.

5. Conclusions

We discovered two new prognostic subtypes associated with immunological dysfunction in PCa patients based on ferroptosis-related genes and found that P4HB downregulation could significantly inhibit the colony formation ability and contributed to cell

apoptosis of PCa cell lines.

Credit author statement

Dechao Feng: Conceived and designed the experiments; Analyzed and interpreted the data; Contributed reagents, materials, analysis tools or data; Wrote the paper. Zhouting Tuo; Jie Wang; Luxia Ye: Conceived and designed the experiments; Performed the experiments; Analyzed and interpreted the data; Contributed reagents, materials, analysis tools or data; Wrote the paper. Dengxiong Li; Ruicheng Wu; Wuran Wei; Yubo Yang; Chi Zhang: Contributed reagents, materials, analysis tools or data; Wrote the paper.

Ethical approval and consent to participate

The authors are accountable for all aspects of the work in ensuring that questions related to the accuracy or integrity of any part of the work are appropriately investigated and resolved.

Consent for publication

Not applicable.

Availability of supporting data

The results showed here are in whole or part based upon data generated by the TCGA Research Network: https://www.cancer.gov/tcga.

Funding

This program was supported by the Luzhou City Science and Technology Bureau (grant number 2021LZXNYDJ10 and 2020LZXNYDJ14), Cooperation Project between the Second People's Hospital of Deyang and Southwest Medical University (2022DYEXNYD002) and program for Talents of Chongqing University Three Gorges Hospital (Grant No. ZX-50010101-2022-347). The funders had no role in the study design, data collection or analysis, preparation of the manuscript, or the decision to publish.

Declaration of competing interest

The authors declare that they have no known competing financial interests or personal relationships that could have appeared to influence the work reported in this paper.

Acknowledgements

We appreciated the Figdraw (www.figdraw.com) and Chengdu Basebiotech Co,Ltd for their assistance in drawing and data process.

Appendix A. Supplementary data

Supplementary data to this article can be found online at https://doi.org/10.1016/j.heliyon.2023.e23495.

References

[1] L. Varisli, V. Tolan, J.H. Cen, S. Vlahopoulos, O. Cen, Dissecting the effects of androgen deprivation therapy on cadherin switching in advanced prostate cancer: a molecular perspective, Oncol. Res. 30 (3) (2022) 137–155.
[2] M.F. Megerian, J.S. Kim, J. Badreddine, S.H. Hong, L.E. Ponsky, J.I. Shin, et al., Melatonin and prostate cancer: anti-tumor roles and therapeutic application, Aging Dis 14 (3) (2023 Jun 1) 840–857.
[3] N. Health Commission Of The People's Republic Of China, National guidelines for diagnosis and treatment of prostate cancer 2022 in China (English version), Chin. J. Cancer Res. 34 (3) (2022 Jun 30) 270–288.
[4] Y. Yang, Comments on National guidelines for diagnosis and treatment of prostate cancer 2022 in China (English version), Chin. J. Cancer Res. 34 (5) (2022 Oct 30) 456–457.
[5] H. Zi, S.H. He, X.Y. Leng, X.F. Xu, Q. Huang, H. Weng, et al., Global, regional, and national burden of kidney, bladder, and prostate cancers and their attributable risk factors, 1990-2019, Mil Med Res 8 (1) (2021 Nov 24) 60.
[6] D. Feng, X. Shi, F. Zhang, Q. Xiong, Q. Wei, L. Yang, Mitochondria dysfunction-mediated molecular subtypes and gene prognostic index for prostate cancer patients undergoing radical prostatectomy or radiotherapy, Front. Oncol. 12 (2022), 858479.
[7] D. Feng, D. Li, X. Shi, Q. Xiong, F. Zhang, Q. Wei, et al., A gene prognostic index from cellular senescence predicting metastasis and radioresistance for prostate cancer, J. Transl. Med. 20 (1) (2022 Jun 3) 252.
[8] D.C. Feng Li D.X., J. Wang, R.C. Wu, C. Zhang, Senescence-associated lncRNAs indicate distinct molecular subtypes associated with prognosis and androgen response in patients with prostate cancer, Acta Materia Medica 2 (3) (2023) 299–309.
[9] J.Y. Wang, G.P. Yu, L. Li, G.W. Lin, D.W. Ye, Early prostate specific antigen decline and its velocity are independent predictive factors for outcomes of mCRPC patients treated with abiraterone acetate, Mil Med Res 9 (1) (2022 Jan 24) 5.

[10] D. Feng, S. Liu, D. Li, P. Han, W. Wei, Analysis of conventional versus advanced pelvic floor muscle training in the management of urinary incontinence after radical prostatectomy: a systematic review and meta-analysis of randomized controlled trials, Transl. Androl. Urol. 9 (5) (2020 Oct) 2031–2045.
[11] D. Feng, X. Shi, Q. Xiong, F. Zhang, D. Li, W. Wei, et al., A ferroptosis-related gene prognostic index associated with biochemical recurrence and radiation resistance for patients with prostate cancer undergoing radical radiotherapy, Front. Cell Dev. Biol. 10 (2022), 803766.
[12] D. Feng, X. Shi, F. Zhang, Q. Xiong, Q. Wei, L. Yang, Energy metabolism-related gene prognostic index predicts biochemical recurrence for patients with prostate cancer undergoing radical prostatectomy, Front. Immunol. 13 (2022), 839362.
[13] D. Feng, Q. Xiong, Q. Wei, L. Yang, Cellular landscape of tumour microenvironment in prostate cancer, Immunology 168 (2) (2023 Feb) 199–202.
[14] S.J. Dixon, K.M. Lemberg, M.R. Lamprecht, R. Skouta, E.M. Zaitsev, C.E. Gleason, et al., Ferroptosis: an iron-dependent form of nonapoptotic cell death, Cell 149 (5) (2012 May 25) 1060–1072.
[15] B.R. Stockwell, Ferroptosis turns 10: emerging mechanisms, physiological functions, and therapeutic applications, Cell 185 (14) (2022 Jul 7) 2401–2421.
[16] C. Lu, C. Tan, H. Ouyang, Z. Chen, Z. Yan, M. Zhang, Ferroptosis in intracerebral hemorrhage: a panoramic perspective of the metabolism, mechanism and theranostics, Aging Dis 13 (5) (2022 Oct 1) 1348–1364.
[17] J. Ju, Y.N. Song, K. Wang, Mechanism of ferroptosis: a potential target for cardiovascular diseases treatment, Aging Dis 12 (1) (2021 Feb) 261–276.
[18] T. Zhao, X. Guo, Y. Sun, Iron accumulation and lipid peroxidation in the aging retina: implication of ferroptosis in age-related macular degeneration, Aging Dis 12 (2) (2021 Apr) 529–551.
[19] S. Wang, W. Wei, N. Ma, Y. Qu, Q. Liu, Molecular mechanisms of ferroptosis and its role in prostate cancer therapy, Crit. Rev. Oncol. Hematol. 176 (2022 Aug), 103732.
[20] N. Zhou, Bao J. FerrDb, A manually curated resource for regulators and markers of ferroptosis and ferroptosis-disease associations, Database (2020 Jan 1) 2020.
[21] M.M. Mortensen, S. Hoyer, A.S. Lynnerup, T.F. Orntoft, K.D. Sorensen, M. Borre, et al., Expression profiling of prostate cancer tissue delineates genes associated with recurrence after prostatectomy, Sci. Rep. 5 (2015 Nov 2), 16018.
[22] R. Kuner, M. Falth, N.C. Pressinotti, J.C. Brase, S.B. Puig, J. Metzger, et al., The maternal embryonic leucine zipper kinase (MELK) is upregulated in high-grade prostate cancer, J. Mol. Med. (Berl.) 91 (2) (2013 Feb) 237–248.
[23] K.L. Penney, J.A. Sinnott, S. Tyekucheva, T. Gerke, I.M. Shui, P. Kraft, et al., Association of prostate cancer risk variants with gene expression in normal and tumor tissue, Cancer Epidemiol. Biomarkers Prev. 24 (1) (2015 Jan) 255–260.
[24] S. Jain, C.A. Lyons, S.M. Walker, S. McQuaid, S.O. Hynes, D.M. Mitchell, et al., Validation of a Metastatic Assay using biopsies to improve risk stratification in patients with prostate cancer treated with radical radiation therapy, Ann. Oncol. 29 (1) (2018 Jan 1) 215–222.
[25] E. Cerami, J. Gao, U. Dogrusoz, B.E. Gross, S.O. Sumer, B.A. Aksoy, et al., The cBio cancer genomics portal: an open platform for exploring multidimensional cancer genomics data, Cancer Discov. 2 (5) (2012 May) 401–404.
[26] D. Feng, F. Zhang, D. Li, X. Shi, Q. Xiong, Q. Wei, et al., Developing an immune-related gene prognostic index associated with progression and providing new insights into the tumor immune microenvironment of prostate cancer, Immunology 166 (2) (2022 Jun) 197–209.
[27] S. Hanzelmann, R. Castelo, J. Guinney, GSVA: gene set variation analysis for microarray and RNA-seq data, BMC Bioinf. 14 (2013 Jan 16) 7.
[28] A. Liberzon, A. Subramanian, R. Pinchback, H. Thorvaldsdóttir, P. Tamayo, J.P. Mesirov, Molecular signatures database (MSigDB) 3.0, Bioinformatics 27 (12) (2011 2011-06-15) 1739–1740.
[29] B. Li, E. Severson, J.C. Pignon, H. Zhao, T. Li, J. Novak, et al., Comprehensive analyses of tumor immunity: implications for cancer immunotherapy, Genome Biol. 17 (1) (2016 Aug 22) 174.
[30] K. Yoshihara, M. Shahmoradgoli, E. Martínez, R. Vegesna, H. Kim, W. Torres-Garcia, et al., Inferring tumour purity and stromal and immune cell admixture from expression data, Nat. Commun. 4 (2013 2013) 2612.
[31] D. Zeng, Z. Ye, R. Shen, G. Yu, J. Wu, Y. Xiong, et al., IOBR: multi-omics immuno-oncology biological research to decode tumor microenvironment and signatures, Front. Immunol. 12 (2021), 687975.
[32] P. Jiang, S. Gu, D. Pan, J. Fu, A. Sahu, X. Hu, et al., Signatures of T cell dysfunction and exclusion predict cancer immunotherapy response, Nat. Med. 24 (10) (2018 Oct) 1550–1558.
[33] T.M. Malta, A. Sokolov, A.J. Gentles, T. Burzykowski, L. Poisson, J.N. Weinstein, et al., Machine learning identifies stemness features associated with oncogenic dedifferentiation, Cell 173 (2) (2018 2018-04-05), 338-54.e15.
[34] V. Thorsson, D.L. Gibbs, S.D. Brown, D. Wolf, D.S. Bortone, T.-H. Ou Yang, et al., The immune landscape of cancer, Immunity 48 (4) (2018 2018-04-17), 812-30.e14.
[35] R. Beroukhim, C.H. Mermel, D. Porter, G. Wei, S. Raychaudhuri, J. Donovan, et al., The landscape of somatic copy-number alteration across human cancers, Nature 463 (7283) (2010 Feb 18) 899–905.
[36] R. Bonneville, M.A. Krook, E.A. Kautto, J. Miya, M.R. Wing, H.-Z. Chen, et al., Landscape of Microsatellite Instability across 39 Cancer Types, vol. 2017, JCO precision oncology, 2017.
[37] Y. Qian, D. Feng, J. Wang, W. Wei, Q. Wei, P. Han, et al., Establishment of cancer-associated fibroblasts-related subtypes and prognostic index for prostate cancer through single-cell and bulk RNA transcriptome, Sci. Rep. 13 (1) (2023 Jun 3) 9016.
[38] D. Feng, J. Wang, X. Shi, D. Li, W. Wei, P. Han, Membrane tension-mediated stiff and soft tumor subtypes closely associated with prognosis for prostate cancer patients, Eur. J. Med. Res. 28 (1) (2023 May 13) 172.
[39] D. Feng, J. Wang, D. Li, R. Wu, W. Wei, C. Zhang, Senescence-associated secretory phenotype constructed detrimental and beneficial subtypes and prognostic index for prostate cancer patients undergoing radical prostatectomy, Discov Oncol 14 (1) (2023 Aug 25) 155.
[40] X. Shi, D. Feng, D. Li, P. Han, L. Yang, W. Wei, A pan-cancer analysis of the oncogenic and immunological roles of apolipoprotein F (APOF) in human cancer, Eur. J. Med. Res. 28 (1) (2023 Jun 14) 190.
[41] D. Feng, X. Shi, W. Zhu, F. Zhang, D. Li, P. Han, et al., A pan-cancer analysis of the oncogenic role of leucine zipper protein 2 in human cancer, Exp. Hematol. Oncol. 11 (1) (2022 Sep 15) 55.
[42] W. Zhu, D. Feng, X. Shi, D. Li, Q. Wei, L. Yang, A pan-cancer analysis of the oncogenic role of zinc finger protein 419 in human cancer, Front. Oncol. 12 (2022), 1042118.
[43] X. Wang, Y. Bai, F. Zhang, Y. Yang, D. Feng, A. Li, et al., Targeted inhibition of P4HB promotes cell sensitivity to gemcitabine in urothelial carcinoma of the bladder, OncoTargets Ther. 13 (2020) 9543–9558.
[44] D. Feng, L. Li, D. Li, R. Wu, W. Zhu, J. Wang, et al., Prolyl 4-hydroxylase subunit beta (P4HB) could serve as a prognostic and radiosensitivity biomarker for prostate cancer patients, Eur. J. Med. Res. 28 (1) (2023 Jul 22) 245.
[45] N. Health Commission Of The People's Republic Of China, National guidelines for diagnosis and treatment of lung cancer 2022 in China (English version), Chin. J. Cancer Res. 34 (3) (2022 Jun 30) 176–206.
[46] N. Health Commission Of The People's Republic Of China, National guidelines for diagnosis and treatment of breast cancer 2022 in China (English version), Chin. J. Cancer Res. 34 (3) (2022 Jun 30) 151–175.
[47] N. Health Commission Of The People's Republic Of China, National guidelines for diagnosis and treatment of pancreatic cancer 2022 in China (English version), Chin. J. Cancer Res. 34 (3) (2022 Jun 30) 238–255.
[48] N. Health Commission Of The People's Republic Of China, National guidelines for diagnosis and treatment of gastric cancer 2022 in China (English version), Chin. J. Cancer Res. 34 (3) (2022 Jun 30) 207–237.
[49] D.C. Feng, W.Z. Zhu, X. Shi, Q. Xiong, J. You, Q. Wei, L. Yang, Identification of senescence-related molecular subtypes and key genes for prostate cancer, Asian J. Androl. 25 (2) (2023 Mar-Apr) 223–229, https://doi.org/10.4103/aja202258. PMID: 36124532; PMCID: PMC10069687.
[50] D. Feng, D. Li, Y. Xiao, R. Wu, J. Wang, C. Zhang, Focal ablation therapy presents promising results for selectively localized prostate cancer patients, Chin. J. Cancer Res. 35 (4) (2023 Aug 30) 424–430, https://doi.org/10.21147/j.issn.1000-9604.2023.04.08. PMID: 37691892; PMCID: PMC10485919.
[51] G Cheng, A Xie, Z Yan, X Zhu, Y Song, T Chen, Nanomedicines for Alzheimer's disease: Therapies based on pathological mechanisms, Brain-X 1 (3) (2023), e27.

[52] A.G. Schwartz, Dehydroepiandrosterone, cancer, and aging, Aging Dis 13 (2) (2022 Apr) 423–432.
[53] W. Shen, J. He, T. Hou, J. Si, S. Chen, Common pathogenetic mechanisms underlying aging and tumor and means of interventions, Aging Dis 13 (4) (2022 Jul 11) 1063–1091.
[54] S. Yuan, C. Fang, W.D. Leng, L. Wu, B.H. Li, X.H. Wang, et al., Oral microbiota in the oral-genitourinary axis: identifying periodontitis as a potential risk of genitourinary cancers, Mil Med Res 8 (1) (2021 Sep 29) 54.
[55] F. Pu, F. Chen, Z. Zhang, D. Shi, B. Zhong, X. Lv, et al., Ferroptosis as a novel form of regulated cell death: implications in the pathogenesis, oncometabolism and treatment of human cancer, Genes Dis 9 (2) (2022 Mar) 347–357.
[56] Y. Yang, X. Lin, Potential relationship between autophagy and ferroptosis in myocardial ischemia/reperfusion injury, Genes Dis 10 (6) (2023 Nov) 2285–2295.
[57] L. Wang, X. Chen, Yan C. Ferroptosis, An emerging therapeutic opportunity for cancer, Genes Dis 9 (2) (2022 Mar) 334–346.
[58] Y. Xie, W. Hou, X. Song, Y. Yu, J. Huang, X. Sun, et al., Ferroptosis: process and function, Cell Death Differ. 23 (3) (2016 Mar) 369–379.
[59] A.M. Battaglia, R. Chirillo, I. Aversa, A. Sacco, F. Costanzo, F. Biamonte, Ferroptosis and cancer: mitochondria meet the "iron maiden" cell death, Cells 9 (6) (2020 Jun 20).
[60] L.S. Simon, Role and regulation of cyclooxygenase-2 during inflammation, Am. J. Med. 106 (5B) (1999 May 31) 37S–42S.
[61] G. Chen, L. Li, H. Tao, Bioinformatics identification of ferroptosis-related biomarkers and therapeutic compounds in ischemic stroke, Front. Neurol. 12 (2021), 745240.
[62] N. Li, W. Wang, H. Zhou, Q. Wu, M. Duan, C. Liu, et al., Ferritinophagy-mediated ferroptosis is involved in sepsis-induced cardiac injury, Free Radic. Biol. Med. 160 (2020 Nov 20) 303–318.
[63] H. Liu, L. Gao, T. Xie, J. Li, T.S. Zhai, Y. Xu, Identification and validation of a prognostic signature for prostate cancer based on ferroptosis-related genes, Front. Oncol. 11 (2021), 623313.
[64] Y. Xu, Y. Liu, K. Li, D. Yuan, S. Yang, L. Zhou, et al., COX-2/PGE2 pathway inhibits the ferroptosis induced by cerebral ischemia reperfusion, Mol. Neurobiol. 59 (3) (2022 Mar) 1619–1631.
[65] V.S. Pereira, B. Alves, J. Waisberg, F. Fonseca, F. Gehrke, Detection of COX-2 in liquid biopsy of patients with prostate cancer, J. Clin. Pathol. 76 (3) (2023 Mar) 189–193.
[66] R. Garg, J.M. Blando, C.J. Perez, P. Lal, M.D. Feldman, E.M. Smyth, et al., COX-2 mediates pro-tumorigenic effects of PKCepsilon in prostate cancer, Oncogene 37 (34) (2018 Aug) 4735–4749.
[67] S. Gupta, M. Srivastava, N. Ahmad, D.G. Bostwick, H. Mukhtar, Over-expression of cyclooxygenase-2 in human prostate adenocarcinoma, Prostate 42 (1) (2000 Jan) 73–78.
[68] J. Tian, F. Guo, Y. Chen, Y. Li, B. Yu, Y. Li, Nanoliposomal formulation encapsulating celecoxib and genistein inhibiting COX-2 pathway and Glut-1 receptors to prevent prostate cancer cell proliferation, Cancer Lett. 448 (2019 Apr 28) 1–10.
[69] C.J. Ko, S.W. Lan, Y.C. Lu, T.S. Cheng, P.F. Lai, C.H. Tsai, et al., Inhibition of cyclooxygenase-2-mediated matriptase activation contributes to the suppression of prostate cancer cell motility and metastasis, Oncogene 36 (32) (2017 Aug 10) 4597–4609.
[70] S. Parakh, J.D. Atkin, Novel roles for protein disulphide isomerase in disease states: a double edged sword? Front. Cell Dev. Biol. 3 (2015) 30.
[71] X. Ma, J. Wang, J. Zhuang, X. Ma, N. Zheng, Y. Song, et al., P4HB modulates epithelial-mesenchymal transition and the beta-catenin/Snail pathway influencing chemoresistance in liver cancer cells, Oncol. Lett. 20 (1) (2020 Jul) 257–265.
[72] Y. Wu, Y. Peng, B. Guan, A. He, K. Yang, S. He, et al., P4HB: a novel diagnostic and prognostic biomarker for bladder carcinoma, Oncol. Lett. 21 (2) (2021 2021-02) 95.
[73] L. Xie, H. Li, L. Zhang, X. Ma, Y. Dang, J. Guo, et al., Autophagy-related gene P4HB: a novel diagnosis and prognosis marker for kidney renal clear cell carcinoma, Aging (Albany NY) 12 (2) (2020 Jan 30) 1828–1842.
[74] C.F. Pan, K. Wei, Z.J. Ma, Y.Z. He, J.J. Huang, Z.Z. Guo, et al., CircP4HB regulates ferroptosis via SLC7A11-mediated glutathione synthesis in lung adenocarcinoma, Transl. Lung Cancer Res. 11 (3) (2022 Mar) 366–380.
[75] J.R. Kovalski, D. Kuzuoglu-Ozturk, D. Ruggero, Protein synthesis control in cancer: selectivity and therapeutic targeting, EMBO J. 41 (8) (2022 Apr 19), e109823.
[76] M.L. Truitt, D. Ruggero, New frontiers in translational control of the cancer genome, Nat. Rev. Cancer 16 (5) (2016 Apr 26) 288–304.
[77] C. Delloye-Bourgeois, D. Goldschneider, A. Paradisi, G. Therizols, S. Belin, S. Hacot, et al., Nucleolar localization of a netrin-1 isoform enhances tumor cell proliferation, Sci. Signal. 5 (236) (2012 Aug 7) ra57.
[78] M. Barna, A. Pusic, O. Zollo, M. Costa, N. Kondrashov, E. Rego, et al., Suppression of Myc oncogenic activity by ribosomal protein haploinsufficiency, Nature 456 (7224) (2008 Dec 18) 971–975.
[79] R. Moreno-Sanchez, S. Rodriguez-Enriquez, A. Marin-Hernandez, E. Saavedra, Energy metabolism in tumor cells, FEBS J. 274 (6) (2007 Mar) 1393–1418.
[80] M.V. Liberti, J.W. Locasale, The warburg effect: how does it benefit cancer cells? Trends Biochem. Sci. 41 (3) (2016 Mar) 211–218.
[81] L.C. Costello, R.B. Franklin, The clinical relevance of the metabolism of prostate cancer; zinc and tumor suppression: connecting the dots, Mol. Cancer 5 (2006 May 15) 17.
[82] S.M. Abbott, K.J. Reid, P.C. Zee, Circadian rhythm sleep-wake disorders, Psychiatr Clin North Am 38 (4) (2015 Dec) 805–823.
[83] M.H. Smolensky, R.C. Hermida, F. Portaluppi, Circadian mechanisms of 24-hour blood pressure regulation and patterning, Sleep Med. Rev. 33 (2017 Jun) 4–16.
[84] M. Baxter, D.W. Ray, Circadian rhythms in innate immunity and stress responses, Immunology 161 (4) (2020 Dec) 261–267.
[85] M.G. Wendeu-Foyet, F. Menegaux, Circadian disruption and prostate cancer risk: an updated review of epidemiological evidences, Cancer Epidemiol. Biomarkers Prev. 26 (7) (2017 Jul) 985–991.
[86] D. Feng, Q. Xiong, F. Zhang, X. Shi, H. Xu, W. Wei, et al., Identification of a novel nomogram to predict progression based on the circadian clock and insights into the tumor immune microenvironment in prostate cancer, Front. Immunol. 13 (2022), 777724.
[87] P. Kaur, N.E. Mohamed, M. Archer, M.G. Figueiro, N. Kyprianou, Impact of circadian rhythms on the development and clinical management of genitourinary cancers, Front. Oncol. 12 (2022), 759153.
[88] J. Liu, M. Yang, R. Kang, D.J. Klionsky, D. Tang, Autophagic degradation of the circadian clock regulator promotes ferroptosis, Autophagy 15 (11) (2019 Nov) 2033–2035.
[89] S.A. Scuderi, M. Lanza, G. Casili, F. Esposito, C. Colarossi, D. Giuffrida, et al., TBK1 inhibitor exerts antiproliferative effect on glioblastoma multiforme cells, Oncol. Res. 28 (7) (2021 Sep 7) 779–790.
[90] D. Robinson, E.M. Van Allen, Y.M. Wu, N. Schultz, R.J. Lonigro, J.M. Mosquera, et al., Integrative clinical genomics of advanced prostate cancer, Cell 162 (2) (2015 Jul 16) 454.
[91] M. Fraser, V.Y. Sabelnykova, T.N. Yamaguchi, L.E. Heisler, J. Livingstone, V. Huang, et al., Genomic hallmarks of localized, non-indolent prostate cancer, Nature 541 (7637) (2017 Jan 19) 359–364.
[92] J. Mateo, G. Seed, C. Bertan, P. Rescigno, D. Dolling, I. Figueiredo, et al., Genomics of lethal prostate cancer at diagnosis and castration resistance, J. Clin. Invest. 130 (4) (2020 Apr 1) 1743–1751.
[93] B. De Laere, S. Oeyen, M. Mayrhofer, T. Whitington, P.J. van Dam, P. Van Oyen, et al., TP53 outperforms other androgen receptor biomarkers to predict abiraterone or enzalutamide outcome in metastatic castration-resistant prostate cancer, Clin. Cancer Res. 25 (6) (2019 Mar 15) 1766–1773.
[94] N. McGranahan, R.A. Burrell, D. Endesfelder, M.R. Novelli, C. Swanton, Cancer chromosomal instability: therapeutic and diagnostic challenges, EMBO Rep. 13 (6) (2012 Jun 1) 528–538.
[95] T.B.K. Watkins, E.L. Lim, M. Petkovic, S. Elizalde, N.J. Birkbak, G.A. Wilson, et al., Pervasive chromosomal instability and karyotype order in tumour evolution, Nature 587 (7832) (2020 Nov) 126–132.
[96] T. Higuchi, M. Nakamura, K. Shimada, E. Ishida, K. Hirao, N. Konishi, HRK inactivation associated with promoter methylation and LOH in prostate cancer, Prostate 68 (1) (2008 Jan 1) 105–113.

[97] B. Wu, X. Lu, H. Shen, X. Yuan, X. Wang, N. Yin, et al., Intratumoral heterogeneity and genetic characteristics of prostate cancer, Int. J. Cancer 146 (12) (2020 Jun 15) 3369–3378.
[98] H. Li, Z.Y. Liu, N. Wu, Y.C. Chen, Q. Cheng, J. Wang, PARP inhibitor resistance: the underlying mechanisms and clinical implications, Mol. Cancer 19 (1) (2020 Jun 20) 107.
[99] L. Nguyen, J. Wmm, A. Van Hoeck, E. Cuppen, Pan-cancer landscape of homologous recombination deficiency, Nat. Commun. 11 (1) (2020 Nov 4) 5584.
[100] D. Sigorski, E. Izycka-Swieszewska, L. Bodnar, Poly(ADP-Ribose) polymerase inhibitors in prostate cancer: molecular mechanisms, and preclinical and clinical data, Targeted Oncol. 15 (6) (2020 Dec) 709–722.
[101] A.M. Elshazly, T.V.V. Nguyen, D.A. Gewirtz, Is autophagy induction by PARP inhibitors a target for therapeutic benefit? Oncol. Res. 30 (1) (2022) 1–12.
[102] C.J. Lord, A. Ashworth, BRCAness revisited, Nat. Rev. Cancer 16 (2) (2016 Feb) 110–120.
[103] R.J. Hause, C.C. Pritchard, J. Shendure, S.J. Salipante, Classification and characterization of microsatellite instability across 18 cancer types, Nat. Med. 22 (11) (2016 Nov) 1342–1350.
[104] P. Zhao, L. Li, X. Jiang, Q. Li, Mismatch repair deficiency/microsatellite instability-high as a predictor for anti-PD-1/PD-L1 immunotherapy efficacy, J. Hematol. Oncol. 12 (1) (2019 May 31) 54.
[105] Q. Jiang, C. Tian, H. Wu, L. Min, H. Chen, L. Chen, et al., Tertiary lymphoid structure patterns predicted anti-PD1 therapeutic responses in gastric cancer, Chin. J. Cancer Res. 34 (4) (2022 Aug 30) 365–382.
[106] Z. Wang, Y. Wang, X. Li, Y. Li, Z. Bu, Z. Li, et al., Correlation between imaging features on computed tomography and combined positive score of PD-L1 expression in patients with gastric cancer, Chin. J. Cancer Res. 34 (5) (2022 Oct 30) 510–518.
[107] D.T. Le, J.N. Uram, H. Wang, B.R. Bartlett, H. Kemberling, A.D. Eyring, et al., PD-1 blockade in tumors with mismatch-repair deficiency, N. Engl. J. Med. 372 (26) (2015 Jun 25) 2509–2520.
[108] W. Wang, M. Green, J.E. Choi, M. Gijon, P.D. Kennedy, J.K. Johnson, et al., CD8(+) T cells regulate tumour ferroptosis during cancer immunotherapy, Nature 569 (7755) (2019 May) 270–274.
[109] T.A. Chan, M. Yarchoan, E. Jaffee, C. Swanton, S.A. Quezada, A. Stenzinger, et al., Development of tumor mutation burden as an immunotherapy biomarker: utility for the oncology clinic, Ann. Oncol.: Official Journal of the European Society for Medical Oncology 30 (1) (2019 2019-01-01) 44–56.
[110] M.M. Gubin, M.N. Artyomov, E.R. Mardis, R.D. Schreiber, Tumor neoantigens: building a framework for personalized cancer immunotherapy, J. Clin. Invest. 125 (9) (2015 Sep) 3413–3421.
[111] J.Y. Wang, W.P. Wang, B7-H4, a promising target for immunotherapy, Cell. Immunol. 347 (2020 Jan), 104008.
[112] H. Li, L. Piao, S. Liu, Y. Cui, Y. Xuan, B7-H4 is a potential prognostic biomarker of prostate cancer, Exp. Mol. Pathol. 114 (2020 Jun), 104406.
[113] M. Janakiram, U.A. Shah, W. Liu, A. Zhao, M.P. Schoenberg, X. Zang, The third group of the B7-CD28 immune checkpoint family: HHLA2, TMIGD2, B7x, and B7-H3, Immunol. Rev. 276 (1) (2017 Mar) 26–39.
[114] M. Janakiram, J.M. Chinai, S. Fineberg, A. Fiser, C. Montagna, R. Medavarapu, et al., Expression, clinical significance, and receptor identification of the newest B7 family member HHLA2 protein, Clin. Cancer Res. 21 (10) (2015 May 15) 2359–2366.
[115] H. Cheng, M. Janakiram, A. Borczuk, J. Lin, W. Qiu, H. Liu, et al., HHLA2, a new immune checkpoint member of the B7 family, is widely expressed in human lung cancer and associated with EGFR mutational status, Clin. Cancer Res. 23 (3) (2017 Feb 1) 825–832.
[116] P. Koirala, M.E. Roth, J. Gill, J.M. Chinai, M.R. Ewart, S. Piperdi, et al., HHLA2, a member of the B7 family, is expressed in human osteosarcoma and is associated with metastases and worse survival, Sci. Rep. 6 (2016 Aug 17), 31154.
[117] J. Zhang, X. Bu, H. Wang, Y. Zhu, Y. Geng, N.T. Nihira, et al., Cyclin D-CDK4 kinase destabilizes PD-L1 via cullin 3-SPOP to control cancer immune surveillance, Nature 553 (7686) (2018 Jan 4) 91–95.
[118] Y. Gong, L. Wang, U. Chippada-Venkata, X. Dai, W.K. Oh, J. Zhu, Constructing Bayesian networks by integrating gene expression and copy number data identifies NLGN4Y as a novel regulator of prostate cancer progression, Oncotarget 7 (42) (2016 Oct 18) 68688–68707.
[119] Y.M. Hu, X.L. Lou, B.Z. Liu, L. Sun, S. Wan, L. Wu, et al., TGF-beta1-regulated miR-3691-3p targets E2F3 and PRDM1 to inhibit prostate cancer progression, Asian J. Androl. 23 (2) (2021 Mar-Apr) 188–196.
[120] Y. Wang, K. Yan, J. Wang, J. Lin, J. Bi, M2 macrophage Co-expression factors correlate with immune phenotype and predict prognosis of bladder cancer, Front. Oncol. 11 (2021), 609334.
[121] J. Zhu, T.A. O'Mara, D. Liu, V.W. Setiawan, D. Glubb, A.B. Spurdle, et al., Associations between genetically predicted circulating protein concentrations and endometrial cancer risk, Cancers 13 (9) (2021 Apr 26).
[122] C.B. Williams, K. Phelps-Polirer, I.P. Dingle, C.J. Williams, M.J. Rhett, S.T. Eblen, et al., HUNK phosphorylates EGFR to regulate breast cancer metastasis, Oncogene 39 (5) (2020 Jan) 1112–1124.
[123] Y. Feng, Y. Gao, J. Yu, G. Jiang, X. Zhang, X. Lin, et al., CCDC85B promotes non-small cell lung cancer cell proliferation and invasion, Mol. Carcinog. 58 (1) (2019 Jan) 126–134.
[124] M. Gentiluomo, G. Capurso, L. Morelli, S. Ermini, C. Pasquali, A. Latiano, et al., Genetically determined telomere length is associated with pancreatic neuroendocrine neoplasms onset, Neuroendocrinology 112 (12) (2022) 1168–1176.
[125] L.B. Hesson, B. Ng, P. Zarzour, S. Srivastava, C.T. Kwok, D. Packham, et al., Integrated genetic, epigenetic, and transcriptional profiling identifies molecular pathways in the development of laterally spreading tumors, Mol. Cancer Res. 14 (12) (2016 Dec) 1217–1228.